
This is an electronic reprint of the original article.
This reprint may differ from the original in pagination and typographic detail.

Author(s): Savin, A. M. & Pekola, Jukka & Flyktman, J. T. & Anthore, A. & Giazotto, F.

Title: Cold electron Josephson transistor

Year: 2004

Version: Final published version

Please cite the original version:

Savin, A. M. & Pekola, Jukka & Flyktman, J. T. & Anthore, A. & Giazotto, F. 2004. Cold electron Josephson transistor. *Applied Physics Letters*. Volume 84, Issue 21. P. 4179-4181. ISSN 0003-6951 (printed). DOI: 10.1063/1.1756192.

Rights: © 2004 American Institute of Physics. This article may be downloaded for personal use only. Any other use requires prior permission of the author and the American Institute of Physics. The following article appeared in *Applied Physics Letters* and may be found at <http://scitation.aip.org/content/aip/journal/apl/84/21/10.1063/1.1756192>

All material supplied via Aaltodoc is protected by copyright and other intellectual property rights, and duplication or sale of all or part of any of the repository collections is not permitted, except that material may be duplicated by you for your research use or educational purposes in electronic or print form. You must obtain permission for any other use. Electronic or print copies may not be offered, whether for sale or otherwise to anyone who is not an authorised user.

Cold electron Josephson transistor

A. M. Savin, J. P. Pekola, J. T. Flyktman, A. Anthore, and F. Giazotto

Citation: *Applied Physics Letters* **84**, 4179 (2004); doi: 10.1063/1.1756192

View online: <http://dx.doi.org/10.1063/1.1756192>

View Table of Contents: <http://scitation.aip.org/content/aip/journal/apl/84/21?ver=pdfcov>

Published by the [AIP Publishing](#)

Articles you may be interested in

[Parallel array of YBa₂Cu₃O_{7- \$\delta\$} superconducting Josephson vortex-flow transistors with high current gains](#)
Appl. Phys. Lett. **103**, 092601 (2013); 10.1063/1.4819461

[Charge sensitivity of the inductive single-electron transistor](#)
Appl. Phys. Lett. **87**, 092502 (2005); 10.1063/1.2034096


[Charge and spin effects in mesoscopic Josephson junctions \(Review\)](#)
Low Temp. Phys. **30**, 554 (2004); 10.1063/1.1789291

[Control of Coulomb blockade in a mesoscopic Josephson junction using single electron tunneling](#)
J. Appl. Phys. **95**, 8059 (2004); 10.1063/1.1751231

[Radio-frequency-induced transport of Cooper pairs in superconducting single electron transistors in a dissipative environment](#)
J. Appl. Phys. **95**, 6325 (2004); 10.1063/1.1713024

The advertisement features a dark red background on the left with the text 'SHARE your expertise in simulation' in white and yellow. On the right, there is a screenshot of the COMSOL software interface showing a 3D simulation of a horn antenna. The interface includes a parameter table and a status bar.

TE11 cutoff frequency (fc):	4.868 Hz
Frequency:	fc*1.2 Hz
Wavelength (λ):	0.5205 m
Flare angle:	17 °
Corrugation thickness:	0.105 m
Corrugation length:	0.155 m
Horn thickness:	0.5 m
Horn length:	4 m
Waveguide length:	1 m
Matching corrugation length:	0.25 m

WITH COMSOL APPS » 

Input waveguide cross pol. ratio: 17.657 %
Output aperture cross pol. ratio: 3.025 %
 Target criterion: passed.

Cold electron Josephson transistor

A. M. Savin,^{a)} J. P. Pekola, J. T. Flyktman, and A. Anthore

Low Temperature Laboratory, Helsinki University of Technology, P.O. Box 2200, FIN-02015 HUT, Finland

F. Giazotto

NEST-INFM and Scuola Normale Superiore, I-56126 Pisa, Italy

(Received 20 February 2004; accepted 7 April 2004; published online 6 May 2004)

A superconductor-normal metal-superconductor mesoscopic Josephson junction has been realized in which the critical current is tuned through normal current injection using a symmetric electron cooler directly connected to the weak link. Both enhancement of the critical current by more than a factor of two, and supercurrent suppression have been achieved by varying the cooler bias. Furthermore, this transistor-like device demonstrates large current gain (~ 20) and low power dissipation. © 2004 American Institute of Physics. [DOI: 10.1063/1.1756192]

Transport dynamics in mesoscopic structures where normal metals (N) are coupled with superconductors (S) are currently the focus of extensive research.^{1,2} This stems mainly from the relevance these systems have both from the fundamental physics point of view and in light of their possible exploitation in nanoelectronics. In diffusive SNS junctions, where the length of the N region exceeds the elastic mean free path, coherent sequential Andreev scattering³ between the superconductors may lead to a continuum spectrum of resonant levels¹ responsible for carrying the supercurrent flow through the structure. The Josephson current is given by supercurrent spectrum weighted by the occupation number of correlated electron-hole pairs that is determined by the quasiparticle energy distribution in the N region of the junction. By changing the latter through current injection from additional *nonsuperconducting* terminals connected to the N region⁴ both supercurrent suppression⁵ as well as its sign reversal (π -transition) were demonstrated.⁶ As predicted in Refs. 7 and 8, the distinctive quasiparticle distribution existing in the N region of a biased SINIS structure (where I stands for an insulating barrier) is also well suited to control the Josephson coupling in a long SNS weak link, allowing either large supercurrent *enhancement* or efficient suppression with respect to equilibrium.

In this letter, we present the implementation and characterization of a four-terminal superconducting structure (see Fig. 1) consisting of a SNS mesoscopic junction integrated with a SINIS electron cooler. A similar device was considered but not successfully operated in Ref. 7. In this transistor, the maximum supercurrent flowing in the SNS junction is controlled by voltage biasing the SINIS line whose N region is shared with the Josephson junction. Low temperature transport measurements show enhancement of the critical current under hot quasiparticle extraction by more than a factor of two with respect to equilibrium. In addition this device demonstrates low power dissipation and large current gain.

The sample (shown in Fig. 1) consists of a Cu island, $0.37 \mu\text{m}$ wide and 30 nm thick, symmetrically connected at its ends via insulating barriers (with normal-state resistance

$\mathcal{R}_T \approx 240 \Omega$) to two 60-nm -thick Al reservoirs, thus realizing a SINIS cooler. The Josephson junction instead consists of an Al/Cu/Al SNS weak link (with normal-state resistance $\mathcal{R}_N = 11.5 \Omega$), whose N region is shared with the SINIS line. The minimum interelectrode separation in the SNS junction of the present device is $L_J \approx 0.4 \mu\text{m}$. The structure was fabricated on a thermally oxidized Si substrate by electron beam lithography and three-angle shadow-mask evaporation. The electrical characterization was performed at different bath temperatures down to 70 mK in a dilution refrigerator. From low-temperature resistance measurements we deduced the Cu diffusion coefficient $D \approx 10 \text{ cm}^2/\text{s}$. This low value of D is probably caused by significant intermixing of the materials at the NS interface leading to the strong reduction of the electron mean free path in the weak link. The Al energy gap, $\Delta = 169 \mu\text{eV}$, was inferred from the low-temperature current-voltage characteristic of the SINIS line (see Fig. 4). The coherence length $\xi_N = \sqrt{\hbar D/\Delta} \approx 62 \text{ nm}$ is then much smaller than L_J , providing the frame of the *long* junction regime.

The experiment consists of sweeping the I_{SNS} current across the SNS junction while measuring its differential re-

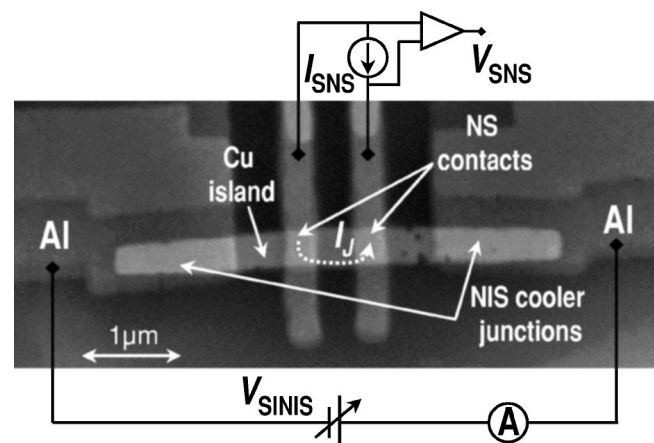


FIG. 1. Scanning electron micrograph of a typical structure including a sketch of the measurement circuit. Two superconducting Al electrodes are connected through insulating barriers to a Cu island to realize a symmetric SINIS electron cooler. The supercurrent I_J in the Al/Cu/Al junction is tuned upon voltage biasing the SINIS control line.

^{a)}Electronic mail: savin@boo.jum.hut.fi

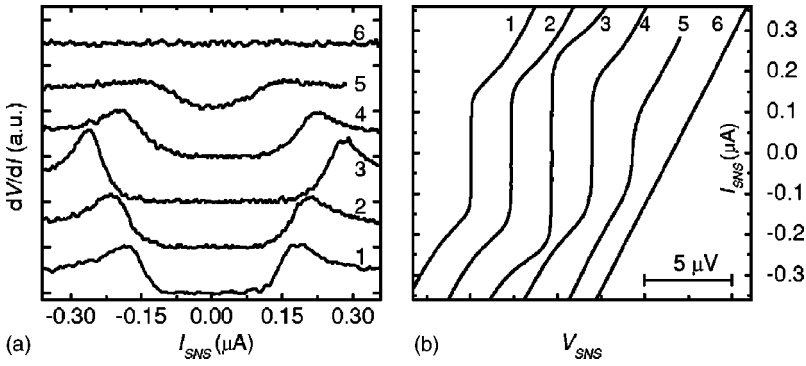


FIG. 2. Selected dV/dI vs I_{SNS} (a) and current–voltage characteristics (b) of the SNS junction at $T_{\text{bath}}=72$ mK for different V_{SINIS} values (all curves are offset for clarity): 1–0, 2–194 μV , 3–300 μV , 4–342 μV , 5–355 μV , 6–938 μV . Curves in (b) were obtained by numerical integration of the corresponding ones in (a).

sistance dV/dI at different values of voltage bias (V_{SINIS}) across the SINIS control line. Figure 2(a) shows a subset of dV/dI vs I_{SNS} characteristics measured at the bath temperature $T_{\text{bath}}=72$ mK for several V_{SINIS} . The curves display a nonhysteretic behavior characteristic for overdamped junctions.⁹ In the case of a SNS weak link the effect of thermal fluctuations on the smearing of the voltage–current characteristic is stronger¹⁰ than predicted by the model for resistively shunted junction.¹¹ We have chosen to define the experimental critical current as the current where the differential resistance reaches $\mathcal{R}_N/2$.¹² Notably, upon increasing V_{SINIS} , the current range where the differential resistance vanishes widens initially, thus reflecting an enhancement of I_J , being maximized at a voltage corresponding to $V_{\text{SINIS}}=300$ $\mu\text{V}\approx 1.8\Delta/e$ ¹³ [curve labeled as 3 in Fig. 2(a)]; then, further increase of bias leads to a monotonic decay and to a complete suppression of I_J at larger voltages [curve labeled as 6 in Fig. 2(a)]. This nonmonotonic behavior is seen in the corresponding I – V curves in Fig. 2(b).

The observed behavior is due to the relation existing between the observable maximum supercurrent I_J and the quasiparticle energy distribution in the weak link. In the present experimental situation of large L_{SINIS} , inelastic electron–electron relaxation forces the electron system to retain a local thermal (quasi)equilibrium. As a consequence, the quasiparticle energy distribution can be described with a Fermi–Dirac function at an *effective* electron temperature T_e . The temperature T_e is determined by the balance between two heat flows:

$$\mathcal{P}(V_{\text{SINIS}}, T_e, T_{\text{bath}}) + \mathcal{P}_{e-\text{bath}}(T_e, T_{\text{bath}}) = 0. \quad (1)$$

The first term accounts for the net heat current \mathcal{P} transferred from the N island to the superconductors upon biasing the SINIS line:¹³

$$\mathcal{P} = \frac{2}{e^2 \mathcal{R}_T} \int_{-\infty}^{\infty} n(E) [f_0(\tilde{E}, T_e) - f_0(E, T_{\text{bath}})] \tilde{E} dE, \quad (2)$$

where $\tilde{E} = E - eV_{\text{SINIS}}/2$, $f_0(E, T)$ is the Fermi–Dirac distribution function and $n(E) = |\text{Re}[(E + i\Gamma)/\sqrt{(E + i\Gamma)^2 - \Delta^2}]|$ is the (smeared by nonzero Γ) BCS density of states of the superconductor.¹⁵ Equation (2) is symmetric in V_{SINIS} , being maximized slightly below $|2\Delta/e|$. The second term accounts for energy transfer from electrons to the phonons of the normal island at the temperature T_{bath} and is equal to $\mathcal{P}_{e-\text{bath}} = \Sigma \mathcal{V}(T_e^5 - T_{\text{bath}}^5)$,¹⁶ where \mathcal{V} is the volume of the N island and $\Sigma \approx 2$ nWK⁻⁵ μm^{-3} for copper.¹³ The temperature T_e in the weak link thus strongly depends on V_{SINIS} and can be

smaller than T_{bath} .¹⁷ At low temperature (i.e., $k_B T_{\text{bath}} \ll \Delta$), in a long SNS junction, I_J is predicted to decrease exponentially as T_e increases¹⁸ in the regime where $k_B T_e \gg E_{\text{Th}} = \hbar D/L_J^2$. Thus, upon biasing the SINIS line, I_J will be changed with respect to equilibrium (i.e., at $V_{\text{SINIS}}=0$), due to the modification of T_e that now differs from T_{bath} .

In Fig. 3(a) we plot the extracted I_J values as a function of V_{SINIS} at three different bath temperatures. For all displayed temperatures, the critical current increases monotonically up to about $V_{\text{SINIS}} \approx 1.8\Delta/e$ as expected from the reduction of T_e by cooling. Then, further increase of bias voltage leads to an efficient supercurrent suppression due to electron heating. The equilibrium critical current (i.e., at $V_{\text{SINIS}}=0$) vs T_{bath} is displayed in Fig. 3(b). The I_J behavior follows a characteristic trend, decreasing upon rising the temperature, but it differs from the temperature dependence predicted by quasiclassical Green-function theory.¹ The discrepancy can be ascribed to the uncertainty in the determination of the actual values of critical current, relatively narrow temperature range where it was observed and thermal decoupling between electrons and bath at temperatures below 200 mK. In Fig. 3, we show the expected critical current dependence on V_{SINIS} at $T_{\text{bath}}=283$ mK obtained from the solution of Eqs. (1) and (2) to determine the effective electron temperature T_e upon biasing the SINIS line, and assuming a linear behavior of the critical current I_J vs T_e below about 350 mK, the slope of the linear dependence being inferred from the measured $I_J(T_{\text{bath}})$. For this calculation, we assumed the already given parameters for the SINIS line and $\Gamma = 1.8 \times 10^{-3} \Delta$ estimated from the ratio ($=\Gamma/\Delta$) of the low-temperature SINIS conductance at low and high bias.¹⁴ The

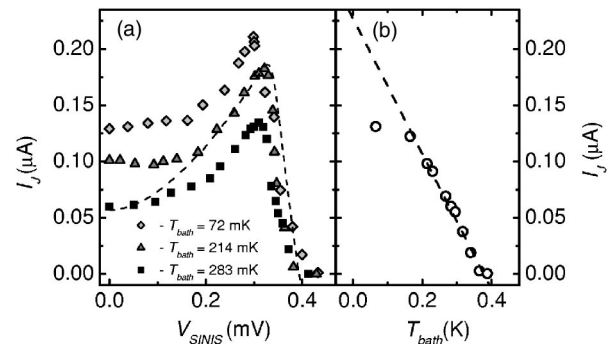


FIG. 3. (a) Critical current I_J vs control voltage V_{SINIS} at three different bath temperatures; (b) equilibrium supercurrent ($V_{\text{SINIS}}=0$) vs bath temperature. Dashed line in (a) represents curve obtained from energy balance Eq. (1) and the linear approximation of $I_J(T_{\text{bath}})$ shown in (b).

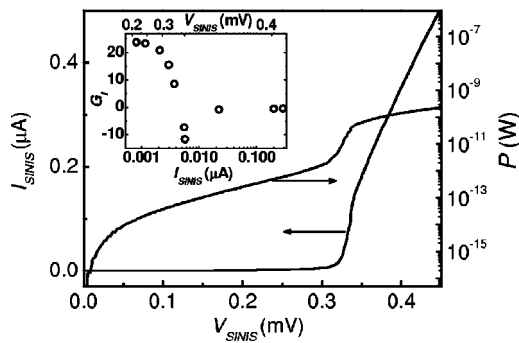


FIG. 4. Current-voltage characteristic (left axis) and power dissipation $P = V_{\text{SINIS}}I_{\text{SINIS}}$ (right axis) of the SINIS line at $T_{\text{bath}}=72$ mK. The inset shows the measured differential current gain G_I against I_{SINIS} at the same temperature (also displayed is the dependence on V_{SINIS}).

resemblance between calculation and experiment is evident although details of the former one are dictated by the I_J dependence on temperature, which we cannot extrapolate reliably. To better characterize our device, we show in Fig. 4 (right axis) the dissipated power P against V_{SINIS} in the SINIS line at $T_{\text{bath}}=72$ mK. The plot reveals that in the bias voltage region of significant critical current enhancement (i.e., in the 200–300 μV bias range) P obtains values of the order of 10^{-13} W, while in the regime of supercurrent suppression (i.e., for $V_{\text{SINIS}}>300$ μV) some tens of pW. This demonstrates the low power dissipation intrinsic to the structure.⁸ The P behavior is directly related to the normal current flow in the control line. The latter is displayed on the left-hand side axis of Fig. 4 and shows that control currents as low as a few nA are necessary to enhance the critical current, while of about 100 nA to suppress it. The differential current gain $G_I = dI_J/dI_{\text{SINIS}}$ against I_{SINIS} is shown in the inset of Fig. 4. Notably, G_I obtains values exceeding 20 in the hot quasiparticle extraction regime, while of about -11 in the voltage region of supercurrent suppression. We note that higher G_I values, as well as lower power dissipation and control currents, could be attained by optimizing the structure design.^{8,14}

In summary, we have demonstrated experimentally control of Josephson coupling under hot quasiparticle extraction in a four-terminal superconducting structure. Our experimen-

tal result shows the potential of a SINIS line as a basis of a promising class of mesoscopic transistors with high current gain.

The authors acknowledge T. T. Heikkilä, F. Carillo, R. Fazio, P. J. Hakonen, F. W. J. Hekking, and F. Taddei for discussions, and Academy of Finland for financial support (TULE Program). One of the authors (F.G.) would like to acknowledge the Large Scale Installation Program ULTI-3 of the European Union for the kind hospitality and for financial support.

- ¹W. Belzig, F. K. Wilhelm, C. Bruder, G. Schön, and A. D. Zaikin, *Superlattices Microstruct.* **25**, 1251 (1999).
- ²C. J. Lambert and R. Raimondi, *J. Phys.: Condens. Matter* **10**, 901 (1998).
- ³A. F. Andreev, *Zh. Eksp. Teor. Fiz.* **46**, 1823 (1964).
- ⁴F. K. Wilhelm, G. Schön, and A. D. Zaikin, *Phys. Rev. Lett.* **81**, 1682 (1998); A. F. Volkov, *ibid.* **74**, 4730 (1995); S.-K. Yip, *Phys. Rev. B* **58**, 5803 (1998).
- ⁵A. F. Morpurgo, T. M. Klapwijk, and B. J. van Wees, *Appl. Phys. Lett.* **72**, 966 (1998).
- ⁶J. J. A. Baselmans, A. F. Morpurgo, B. J. van Wees, and T. M. Klapwijk, *Nature (London)* **397**, 43 (1999); R. Shaikhaidarov, A. F. Volkov, H. Takayanagi, V. T. Petrushov, and P. Delsing, *Phys. Rev. B* **62**, R14649 (2000); J. Huang, F. Pierre, T. T. Heikkilä, F. K. Wilhelm, and N. O. Birge, *ibid.* **66**, 020507 (2002).
- ⁷J. J. A. Baselmans, Ph.D. thesis, University of Groningen, The Netherlands, 2002.
- ⁸F. Giazotto, F. Taddei, T. T. Heikkilä, R. Fazio, and F. Beltram, *Appl. Phys. Lett.* **83**, 2877 (2003).
- ⁹K. K. Likharev, *Rev. Mod. Phys.* **51**, 101 (1979).
- ¹⁰T. Hoss, C. Strunk, T. Nussbaumer, R. Huber, U. Staufner, and C. Schönenberger, *Phys. Rev. B* **62**, 4079 (2000).
- ¹¹V. Ambegaokar and B. I. Halperin, *Phys. Rev. Lett.* **22**, 1364 (1969).
- ¹²P. Dubos, H. Courtois, B. Pannetier, F. K. Wilhelm, A. D. Zaikin, and G. Schön, *Phys. Rev. B* **63**, 064502 (2001).
- ¹³M. M. Leivo, J. P. Pekola, and D. V. Averin, *Appl. Phys. Lett.* **68**, 1996 (1996).
- ¹⁴J. P. Pekola, T. T. Heikkilä, A. M. Savin, J. T. Flyktman, F. Giazotto, and F. W. J. Hekking, *Phys. Rev. Lett.* **92**, 056804 (2004).
- ¹⁵The parameter Γ allows quasiparticle states within the energy gap Δ (Ref. 14).
- ¹⁶F. C. Wellstood, C. Urbina, and J. Clarke, *Phys. Rev. B* **49**, 5942 (1994).
- ¹⁷M. L. Roukes, M. R. Freeman, R. S. Germain, and R. C. Richardson, *Phys. Rev. Lett.* **55**, 422 (1985).
- ¹⁸A. D. Zaikin and G. F. Zharkov, *Sov. J. Low Temp. Phys.* **7**, 184 (1981); F. K. Wilhelm, A. D. Zaikin, and G. Schön, *J. Low Temp. Phys.* **106**, 305 (1997).